SAND2011-8713 C

SAND2011-8713C

Time Encoded Fast Neutron/Gamma Imager for Large Standoff SNM Detection

Peter Marleau, James Brennan, Erik Brubaker, Mark Gerling, Aaron Nowack, Patricia Schuster, John Steele

***Abstract*– Passive detection of special nuclear material (SNM) at long range or under heavy shielding can only be directly achieved by observing the penetrating neutral particles that it emits: gamma rays and neutrons in the MeV energy range. The ultimate SNM standoff detector system would have sensitivity to both gamma and neutron radiation, a large area and high efficiency to capture as many signal particles as possible, and good discrimination against background particles via directional and energy information. We are exploring the use of time-modulated collimators that may lead to practical gamma-neutron imaging detector systems that are highly efficient with the potential to exhibit simultaneously high angular and energy resolution. We will present results from a large standoff SNM detection demonstration using a prototype high sensitivity time encoded modulation imager.**

I. Introduction

TIME-CODED apertures were introduced as a technique for gamma ray imaging in medical detectors in the 1970s. Despite promising conclusions in these initial papers on the subject, time-coded apertures have not become a standard technique in medical imagers, possibly because of the difficulties presented by imaging in the near-field regime (1)(2).

Outside of medical imaging, there has been limited work on time-encoding radiation detectors. The Rotating Modulation Collimator (RMC) is the exception and has seen application in both astrophysics and security applications (3)(4).

The RMC demonstrates several advantages of the time-encoding technique: imaging with a single non-position-sensitive detector, good angular resolution, and the absence of artifacts arising from un-attenuated background events. However, the RMC has a fundamentally limited field of view, as well as a geometrical efficiency that is lower than a typical 50% open coded aperture imager (5). Additionally, although an RMC sensitive to thermal neutrons has been investigated; fast neutrons are inherently unsuited to an RMC since the thick collimators needed to attenuate them would severely impact their efficiency. We have pursued a more general application of time modulation to the SNM detection problem that is highly efficient, scalable, and applicable to fast neutron detection.

In an ideal situation, a properly selected coded aperture imager will provide artifact-free reconstruction (6). But non-uniformities, which induce reconstruction artifacts, are very difficult to suppress in a real system. The non-uniformities can arise either from variations in the background field at the image plane due to the local environment or the detector shielding configuration, or from variations in the detector calibrations. We have concluded that converting the spatial modulation of a traditional coded aperture imager to time modulation will maintain the imaging performance of the ideal coded aperture, while simplifying the system design and increasing robustness to local variations in the background field.

All authors are with Sandia National Laboratories, Livermore, CA 94550 USA.

II. Prototype number 1

Last year we simulated, designed, and built a simple conceptual detector design in order to demonstrate the feasibility of a time-encoding collimator (7). Dubbed LIGHTHOUSE, this imager consists of a single central detector, 5” high, 5” radius liquid scintillator (EJ301) filled aluminum cell coupled to a 5” photomultiplier tube (PMT) placed at the center of a series of mask bars arranged in a URA pattern and wrapped into a circle. Fig 1 is a photograph of the completed prototype detector. The mask is arranged in a 31 element URA pattern and constructed from 3.5”×3.5”×27” HDPE bars. The mask bars mount to a steel hoop and axle attached to an aluminum frame by a single bearing. A small electric motor drives the rotation of the mask by sprockets and chain. A digital encoder in the motor is used to update the angular position of the mask as it rotates. The encoded position was included in the data stream by the DAQ and used in offline analysis.

Because of the nature of the nature of the time encoded imager, the radiation detection method (central detector) is completely decoupled from the signal modulator (rotating mask). This allowed us to evaluate different central detectors with relative ease. We built and evaluated several such detectors, but settled on a liquid organic scintillator filled 5” diameter by 5” high aluminum cell coupled to a 5” diameter Hamamatsu PMT. The fast neutron interaction rate is plotted as a function of encoder position modulo a single rotation. This rate vs. angular position is equivalent to the spatial modulation that would be measured at the image plane of a 1D coded aperture imager.

Figure 1: Photograph of the prototype time encoded imager. The 5" diameter LOS cell is inside the box at the center.

The neutron modulation as a function of angular position can be seen in Fig. 2 (top). Fig. 2 (bottom) shows the results of the application of a Maximum Likelihood Estimator Maximize (MLEM) imaging reconstruction technique (8). This figure demonstrates the feasibility of this novel new imaging technique for the first time.

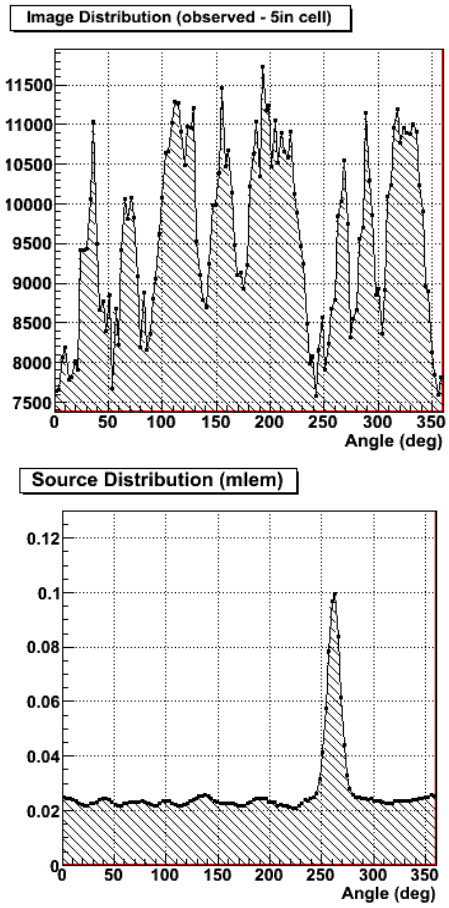

Figure 2: Neutron counts as a function of azimuth angle (arbitrary phase) of the 5" diameter detector (top) and the result of an MLEM image reconstruction (right) (vertical axis is in neutrons per second).

III. The PRISM concept

The concept for this work was originally intended to extend the proof of concept described in the previous section to create a larger and more efficient "LIGHTHOUSE" type imager. The target application is to detect and locate special nuclear material (SNM) at large stand-off distances. Toward this goal, we designed a very large central detector (22 inches diameter x 22 inches depth). However, it was quickly realized that portability constraints would greatly limit the performance of such a detector. In order to fit a rotating mask into a transportable container of reasonable size (~8 feet across), the number of mask elements that encircle the central detector would need to be constrained to achieve an aperture size comparable to the large diameter of the central detector, constraining the angular resolution of the imager. In addition, the mass of a rotating mask this size would lead to some engineering challenges. In summary, though applications certainly exist where this concept is appropriate, a scaled up version of LIGHTHOUSE was proving to be less than practical.

Therefore, we created a new concept based on time encoded imaging that does not require large masses of shielding material. The Portable Rotating Imager using Self Modulation (PRISM) is comprised of only a few detectors that rotate around each other on a common axis. Because the material of adjacent detectors is used to attenuate the signal in any one detector there is no need for the large amounts of extra material required for the LIGHTHOUSE mask. The footprint and overall mass of the imager is thus reduced to the size and mass of the detectors alone.

This leads to a much more efficient and compact imager, however the imaging properties of the URA mask are lost. There is no longer a mathematical guarantee that a point source will reconstruct with little or no artifact, but this design allows for much more detector material in the volume allotted to the imager. Thus for the same dwell time, the PRISM detector will collect greater statistics which may overcome its lack in image quality on a per event basis. All of these factors inspired us to design and construct a number of large liquid scintillator detectors to field in a large stand-off demonstration.

IV. Detector Design

Twelve inch diameter steel cans were designed to house an assembly that holds Photonis XP1802 9 inch diameter PMTs in direct contact with ~27 liters of liquid organic scintillator EJ-309 (8) 15" above the bottom of the can. A small argon filled expansion chamber above the PMT holder (seen in Figure 3) allows the scintillator to expand with temperature as well as providing a place for excess scintillator to move as the detectors rotate without changing the active detector volume. The assembly is held into place with a piston that is sealed airtight with double o-rings. The end of the PMT is passed through the piston and sealed with a third o-ring so that the electronic signal can be passed out through the base and high voltage passed in through the voltage divider. The entire

assembly is then made light tight with a lid that bolts down onto the top of the piston.

The signals from the 4 detectors are digitized by an SIS3350 4 channel 500 Megasample/second 12-bit digitizer card (9) and read out to a Windows PC using custom data acquisition software.

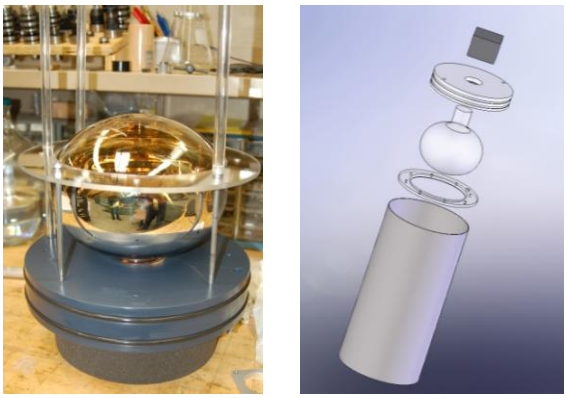

Figure 3: (left) Photograph of the PMT assembly before insertion into the liquid scintillator cell. (right) Exploded view of the design of the liquid scintillator cell showing the steel can, PMT holder, PMT, piston with o-ring seal and PMT base.

Four detectors were assembled and tested. Each exhibited excellent detection response and pulse shape discrimination (PSD). The physical cross-sectional area presented to an SNM source from the side of a single fully assembled cell is ~1160 cm^2, and Monte Carlo simulations indicate that even with reasonable assumptions about the minimum energy detection threshold (160 keV electron equivalent), a fission neutron efficiency of greater than 90% might be expected. However, once inefficiencies due to analysis cuts on PSD are introduced the true efficiency is likely to be lower.

V. Demonstration and Results

The imager point source response as a function of rotation angle was extensively modeled using MCNP-PoliMi (10). Various detector orientations and placements were simulated and evaluated. The best performing model was a three detector design with the shortest radius configuration. As seen in Figure 4, the detectors were mounted to a turntable that is controlled by the data acquisition system by Ethernet. The drive motor includes a shaft encoder which is polled once per second to track the orientation of the detectors through the course of the measurements. The detectors were oscillated through +/- 190 degrees with a period of 360 seconds.

The detectors and turntable were installed inside an insulated and air-conditioned trailer. The trailer was parked in a large open field at Sandia National Laboratories, California. A Cf-252 neutron source was positioned in several locations in the field to the east of the detectors.

Figure 4: The three PRISM detectors mounted to the turn table.

In the first of several imaging demonstrations, a Cf252 neutron source with a neutron emission rate consistent with an IAEA significant quantity of weapons grade plutonium (11) was positioned in three different locations in the field adjacent to the detector trailer. As seen in Figure 5, the source was positioned at a distance of 10 meters (35 feet) at positions approximately 50 degrees apart.

The measured counts per second in a single detector are shown in Figure 6 (left) and the MLEM reconstruction of the source distributions are shown in Figure 6 (right) for the three source positions shown in Figure 5. The modulation as a function of angle due to the attenuation of the other two detectors as they are rotated is readily apparent. These images indicate the presence of a point source in the appropriate locations; separated by 50 degrees as expected. Each run represents approximately 90 seconds of live time and the result is inconsistent with background with a significance of 30 sigma.

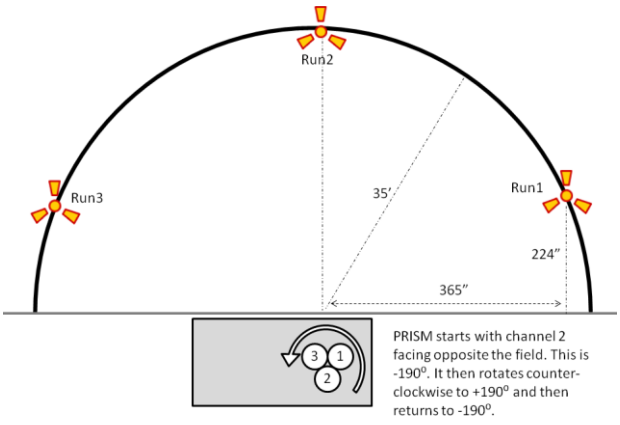

Figure 5: Illustration of the PRISM detector in the trailer (bottom) and the three locations of the Cf252 source.

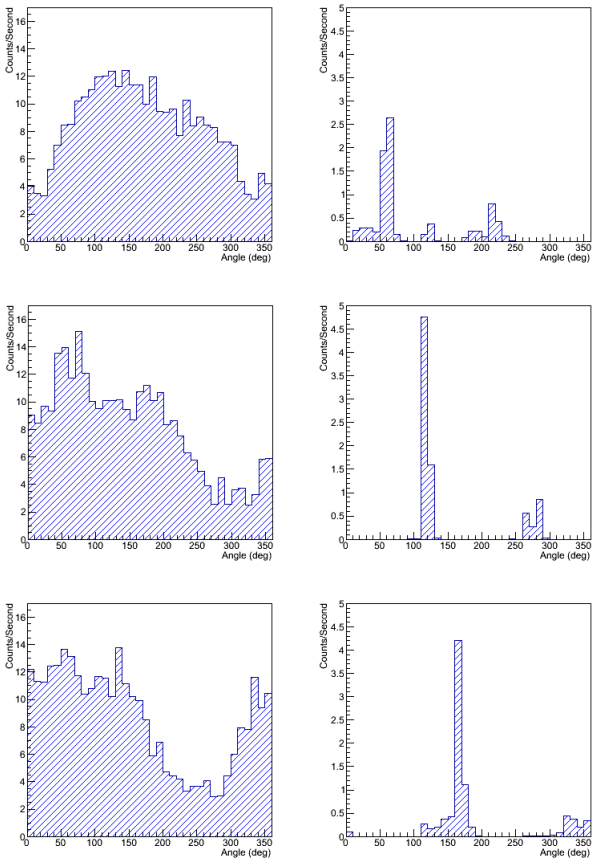

Figure 6: The measured neutron rates in a single detector (left) and MLEM reconstructed source distribution (right) for the 3 source positions labeled Run 1 (top), Run 2 (middle), and Run3 (bottom) in Figure 5.

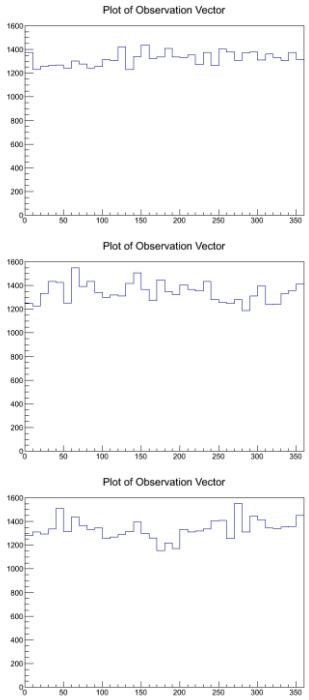

Figure 7: The measured neutron rates as a function of rotation angle for the three detectors

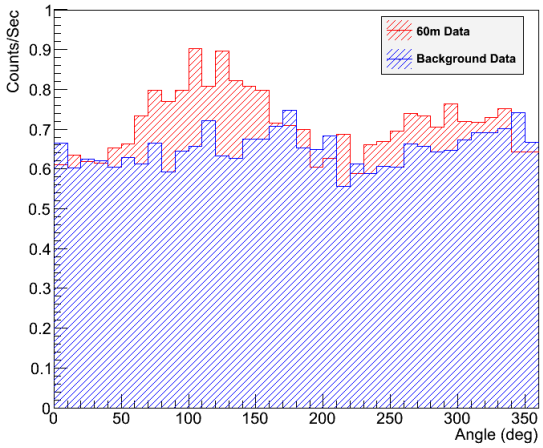

Figure 8: The MLEM reconstructed source distribution for the Cf252 source at 60 meters (red) and background (blue).

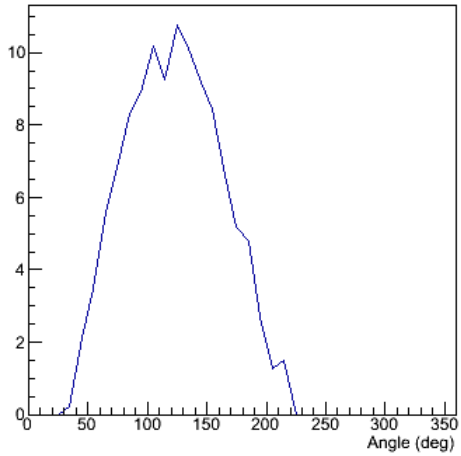

Figure 9: The result of a point source hypothesis test. The vertical axis is the significance of the hypothesis that a single point source is present at each angle given the measured background distribution.

We next moved the source to positions at 60 meters. The measured modulation is shown in Figure 7 (total live time of ~80 minutes) and the reconstructed image is shown in Figure 8 for the source at 60 meters (red) and for background (blue). By applying a point source hypothesis test on the data, we have determined that this measurement is consistent with a point source response centered at the correct source location with 10 sigma significance over the assumption of background alone (Figure 9). This detection is somewhat worse than the performance predicted by Monte Carlo simulations. This is most likely due to systematic shifts in gain as a function of rotation angle due to the PMT orientation in the earth's magnetic field. Future work will include improvements in the magnetic shielding of the PMTs.

ACKNOWLEDGMENT

This work was supported by Laboratory Directed Research and Development (LDRD) at Sandia National Laboratories.

Sandia National Laboratories is a multi-program laboratory managed and operated by Sandia Corporation, a wholly owned subsidiary of Lockheed Martin Corporation, for the U.S.

Department of Energy's National Nuclear Security Administration under Contract DE-AC04-94AL85000. SAND Number 2011-8713 C.

REFERENCES

1. *Digital Tomographic Imaging with Time-Modulated Pseudorandom Coded Aperture and Anger Camera.* **Koral, Kenneth FW, Leslie Rogers, and Glenn F Knoll.** 5, 1974, Journal of Nuclear Medicine, Vol. 16, pp. 402-413.
2. *Gamma-Ray Imaging with Stochastic Apertures.* **May, Randall S, Ziya Akcasu, and Glenn F Knoll.** 11, 1974, Applied Optics, Vol. 13.
3. *The RHESSI imaging concept.* **Hurford, G J, E J Schmahl, R A Schwartz, A J Conway, M J Aschwanden, A Csillaghy, B R Dennis, et al.** 1-2, 2002, Solar Physics , Vol. 210.
4. *A rotating modulation imager for locating mid-range point sources.* **Kowash, B.R., D.K. Wehe, and J.A. Fessler.** 2, 2009, Nuclear Instruments and Methods in Physics Research Section A, Vol. 602.
5. *Thermal neutron imaging with a Rotationally Modulated Collimator (RMC).* **Boyce, Nathan O., Benjamin R. Kowash, and David K. Wehe.** Orlando : s.n., 2009. IEEE Nuclear Science Symposium. pp. 1129-1133.
6. *Coded aperture imaging with uniformly redundant arrays.* **Fenimore, E. E., and T. M. Cannon.** 3, 1978, Applied Optics, Vol. 17.
7. *Results from the Coded Aperture Neutron Imaging System.* **Marleau, P., Brennan, J., Brubaker, E., Steele, J.** Knoxville : s.n., 2010. IEEE Nuclear Science Symposium.
8. **Eljen.** EJ-309 data sheet. [Online] http://www.eljentechnology.com/datasheets/EJ309%20data%20sheet.pdf.
9. **SIS.** SIS3350 data sheet. [Online] http://www.struck.de/sis3350.htm.
10. *MCNP-PoliMi: A Monte Carlo Code for Correlation Measurements.* **Pozzi, S. A., Padovani, E., Marseguerra, M.** 2003, Nucl. Instr. and Meth. A, Vol. 513, pp. 550-558.
11. *IAEA Safeguards Glossary.* **IAEA.** Vienna, Austria : International Verification, 2002, Vol. 3. Table-II and paragraph 3.14.